

© 2023 IEEE. Personal use of this material is permitted. Permission from IEEE must be obtained for all other uses, in any current or future media, including reprinting/republishing this material for advertising or promotional purposes, creating new collective works, for resale or redistribution to servers or lists, or reuse of any copyrighted component of this work in other works.

M. A. Ahrazoğlu, S. Aseem Ul Islam, A. Goel and D. S. Bernstein, "Vibrational Stabilization of the Kapitza Pendulum Using Model Predictive Control with Constrained Base Displacement," 2023 American Control Conference (ACC), San Diego, CA, USA, 2023, pp. 2640-2645, doi: 10.23919/ACC55779.2023.10156185.

<https://doi.org/10.23919/ACC55779.2023.10156185>

Access to this work was provided by the University of Maryland, Baltimore County (UMBC) ScholarWorks@UMBC digital repository on the Maryland Shared Open Access (MD-SOAR) platform.

Please provide feedback

Please support the ScholarWorks@UMBC repository by emailing scholarworks-group@umbc.edu and telling us what having access to this work means to you and why it's important to you. Thank you.

Vibrational Stabilization of the Kapitza Pendulum Using Model Predictive Control with Constrained Base Displacement

M. Akif Ahrazoğlu, Syed Aseem Ul Islam, Ankit Goel, and Dennis S. Bernstein

Abstract—It is well known that, for some systems, stabilization can be achieved by open-loop control in the form of high-frequency vibrations. Vibrational control is attractive since it requires no sensors. On the other hand, however, vibrational control requires careful selection of the frequency and amplitude of the input. The present paper is aimed at understanding the robustness of vibrational control and the required control effort by applying nonlinear model predictive control to the classical Kapitza pendulum. A numerical investigation shows that closed-loop control using nonlinear model predictive control is significantly more efficient than open-loop vibrational control with respect to signal power.

I. INTRODUCTION

Although stabilization is an invaluable benefit of feedback, it is well known that, for some systems, stabilization can be achieved by open-loop controller in the form of high-frequency vibrations. This phenomenon was first analyzed by A. Stephenson in 1908 within the context of the inverted pendulum with periodic vertical base acceleration and further analyzed in 1951 by P. L. Kapitza. Vibrational stabilization has subsequently been applied to diverse applications, and it has been observed in natural systems such as the flight of hummingbirds and fruit flies [1]. A detailed overview of vibrational stabilization is given in [2]. Vibrational stabilization of the Kapitza pendulum (KP) has been widely studied within the framework of the Mathieu equation [3], [4], [5], [6], [7], [8]. A summary of various techniques applied to this problem along with intuitive explanations are given in [9].

As noted in [2], averaging theory analysis of KP [10], [11] applies to the damped case; the undamped KP is not open-loop stabilizable. As pointed out in [2], the qualitative nature of averaging theory provides no analytical guarantees of stabilization for stability for specific choices of amplitude and frequency. These are provided, however, by means of the Ince-Strutt diagram, which shows regions of stability and instability for the linearized system in terms of nondimensionalized parameters.

The present paper revisits the problem of stabilizing KP from a feedback control perspective. Although feedback control is far more demanding than open-loop control in terms of real-time sensing and computation, there are several reasons to pursue this approach. First, as already noted, the convergence of the angle of the undamped KP to zero is

impossible, and thus low levels of damping are potentially problematic. Next, it may be difficult in practice to determine a sinusoidal amplitude and frequency for which stabilization is guaranteed. Furthermore, vibrational stabilization may be inefficient in the sense that, near the vertical equilibrium angle, the amount of control signal power expended may be excessive. Finally, KP provides a nonlinear benchmark problem for assessing the effectiveness of nonlinear feedback control techniques.

In the present paper, we apply model predictive control to KP. A novel aspect of this study is the fact that double integration of a periodic base acceleration input may lead to divergence of the base displacement. For example, double integration of $\sin t$ yields $t - \sin t$, which is unbounded. In physical experiments, the periodic base displacement is constrained by the mechanical system, and thus the corresponding base acceleration has a periodic and thus bounded double integral. Regardless of whether the vertical acceleration of the base is given by an open-loop or closed-loop control law, physical requirements demand that the corresponding base displacement be bounded. The present paper thus accounts for a mechanical base-displacement constraint, which is not considered in the classical analysis.

The need to enforce a base-displacement constraint motivates the use of model predictive control. Since KP is nonlinear, we require an implementation of nonlinear model predictive control. To this end, we use a nonlinear model predictive control technique based on linearization and discretization centered about predicted trajectories, and we use quadratic programming to solve the constrained linear optimization problem at each step. The main contribution of the present paper is a numerical investigation of the feasibility and effectiveness of nonlinear model predictive control for feedback control of KP, including a comparison of the effectiveness of closed-loop control as compared to vibrational open-loop control.

II. MODELING OF THE KAPITZA PENDULUM

A. Equations of Motion

KP is an inverted pendulum that can be stabilized by vertical excitation of the base. In this paper, KP is assumed to consist of a massless rod with tip mass m . The dynamics of KP are given by

$$m(l\ddot{\theta} + a_v \sin \theta) = mg \sin \theta - b(l\dot{\theta} - v_v \sin \theta), \quad (1)$$

where m is the mass of the bob, $g = 9.81 \text{ m/s}^2$ is the acceleration due to gravity, l is the length of the rod, b is the coefficient of rotational viscous damping at the pin joint

M. Akif Ahrazoğlu, Syed Aseem Ul Islam, and Dennis S. Bernstein are with the Department of Aerospace Engineering, University of Michigan, Ann Arbor, MI, USA. {mahrazog, aseemisl, dsbaero}@umich.edu, and Ankit Goel is with the Department of Mechanical Engineer, University of Maryland, Baltimore County, MD, USA. ankgoel@umbc.edu

at the base P, v_v and a_v are the speed and acceleration of P in the z direction, respectively, and θ is the angle between the positive vertical axis and the rod. Defining $x_1 \triangleq \theta$, $x_2 \triangleq \dot{\theta}$, $x_3 \triangleq z$, $x_4 \triangleq \dot{z}$, $u \triangleq a_v$, so that $v_v = \dot{z}$, we can express (1) as

$$\dot{x}_1 = x_2, \quad (2)$$

$$\dot{x}_2 = \frac{g}{l} \sin x_1 - \frac{b}{m} x_2 + \frac{bx_4}{ml} \sin x_1 - \frac{1}{l} (\sin x_1) u, \quad (3)$$

$$\dot{x}_3 = x_4, \quad \dot{x}_4 = u. \quad (4)$$

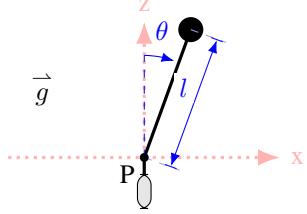


Fig. 1: The Kapitza pendulum.

In the absence of damping, it can be shown that setting $u(t) = a_v(t) \equiv g$ and $x_2(0) = \dot{\theta}(0) = 0$ in (2)–(4) yields equilibria for all values of $x_1(0) = \theta(0)$. This corresponds to the pendulum in free fall and thus unbounded vertical displacement z . In order to preclude the free-fall-stabilization solution, we consider constraints on the vertical displacement z of P.

III. OPEN-LOOP CONTROL OF THE KAPITZA PENDULUM

A. Stability Analysis for Open-loop Control

It is shown in [12] that KP under vibrational stabilization (VS) has an asymptotically stable periodic orbit, while [11] shows that KP exhibits an exponentially stable 2π -periodic solution. Assume that the base acceleration is $A\omega^2 \cos \omega t$, where A is the vibration displacement and ω is the vibration frequency. Defining

$$\varepsilon \triangleq \frac{A}{l}, \quad \omega_0 \triangleq \sqrt{\frac{g}{l}}, \quad \Omega \triangleq \frac{\omega}{\omega_0}, \quad Q \triangleq \frac{\omega_0 m l^2}{b}, \quad (5)$$

we can express (1) as

$$\frac{d^2 \theta}{d\tau^2} + \frac{1}{Q} \frac{d\theta}{d\tau} + \left(\frac{-1}{\Omega^2} + \frac{A}{l} \cos \tau \right) \sin \theta = 0. \quad (6)$$

Next, defining

$$\mu \triangleq \frac{1}{\Omega Q}, \quad \delta \triangleq \frac{-1}{\Omega^2}, \quad (7)$$

and using the small-angle approximation for θ in (6) yields

$$\frac{d^2 \theta}{d\tau^2} + \mu \frac{d\theta}{d\tau} + (\delta + \varepsilon \cos \tau) \theta = 0, \quad (8)$$

which is a Mathieu equation. As shown in [7], the Mathieu equation (8) can be used to construct the Ince-Strutt stability diagram shown in Figure 2, which determines stabilizing values of (ε, δ) .

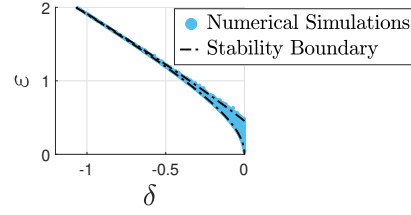


Fig. 2: Ince-Strutt stability diagram, which shows the stability boundary of one region ($\varepsilon \leq 2$) of KP without damping [13] for which the response does not diverge.

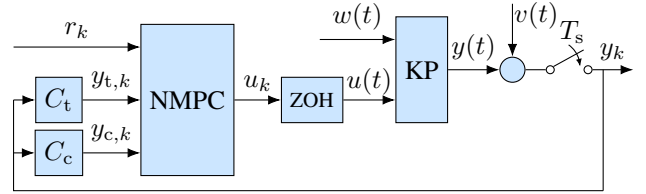


Fig. 3: Sampled-data feedback control architecture.

IV. CONTROL ARCHITECTURE AND OBJECTIVES

In Figure 3, let a representation of KP be given by

$$\dot{x}(t) = f[x(t), u(t), w(t)], \quad (9)$$

$$y(t) = g[x(t), u(t), w(t)], \quad (10)$$

where $x(t) \in \mathbb{R}^n$ is the state given by (2)–(4), $u(t) \in \mathbb{R}^m$ is the control, $w(t) \in \mathbb{R}^{l_w}$ is the disturbance, and $y(t) \in \mathbb{R}^p$ is the output. For simplicity, the disturbance $w(t)$ is assumed to be piecewise constant within each interval kT_s to $(k+1)T_s$, at the value w_k , where $T_s > 0$. We consider disturbance torques, and thus $\frac{w(t)}{ml^2}$ is added to (3). The measurement $y(t)$ of KP is corrupted by sensor noise $v(t)$. The sample operation yields $y_k \triangleq y(kT_s) + v_k$, where $v_k \triangleq v(kT_s) \in \mathbb{R}^p$ is the sampled sensor noise and T_s is the sampling time. In order to facilitate state estimation we assume that y_k is available at 10 time instants within each sample period. For all $k \geq 0$ and $i = 0, \dots, 9$, these measurements are denoted by $y_{k,i} \triangleq y[(k-1)T_s + i\frac{T_s}{10}] + v_k$. The performance objective is to require that $y_{t,k} \triangleq C_t y_k \in \mathbb{R}^{p_t}$ follow the commanded trajectory $r_k \in \mathbb{R}^{p_t}$, where $C_t \in \mathbb{R}^{p_t \times p}$. The inequality constraint objective is to satisfy the constraint $C y_{c,k} + \mathcal{D} \leq 0_{n_c \times 1}$, where $y_{c,k} \triangleq C_c y_k \in \mathbb{R}^{p_c \times p}$ and $\mathcal{C} \in \mathbb{R}^{n_c \times p_c}$ and $\mathcal{D} \in \mathbb{R}^{n_c}$.

To reflect physical control constraints we require that $u_{\min} \leq u_k \leq u_{\max}$, where $u_{\min} \in \mathbb{R}^m, u_{\max} \in \mathbb{R}^m$ are vectors of the minimum and maximum control magnitudes, respectively, and $\Delta u_{\min} \leq u_k - u_{k-1} \leq \Delta u_{\max}$, where $\Delta u_{\min} \in \mathbb{R}^m, \Delta u_{\max} \in \mathbb{R}^m$ are vectors of minimum and maximum control move sizes, respectively. For KP the vertical displacement z has constraints of the form $-z_{\lim} \leq z_k \leq z_{\lim}$, where $z_k \triangleq x_3(kT_s) = z(kT_s)$. Thus, we assume that measurements of x_3 are available. As shown in Figure 3, the inputs to nonlinear model predictive control (NMPC) controller are the command r_k , the tracking output $y_{t,k}$, and the constrained output $y_{c,k}$, which are used by NMPC to produce $u_k \in \mathbb{R}^m$ at each step k .

V. OUTPUT-FEEDBACK NONLINEAR MODEL PREDICTIVE CONTROL

A. Nonuniform Prediction Horizon

At step k , the prediction horizon is defined by $t_{s,1}, \dots, t_{s,\ell}$, which divide the prediction horizon over ℓ possibly unequal steps. In particular, for all $i = 1, \dots, \ell$, the predicted control sequence is given by $u_{1|k}, \dots, u_{\ell|k} \in \mathbb{R}^m$. We define the applied control at the next step as $u_{k+1} \triangleq u_{1|k}$.

B. Linearization and Discretization

We linearize the nonlinear dynamics (9) and (10) centered at $(\bar{x}_{1|k}, \bar{u}_{1|k}), \dots, (\bar{x}_{\ell|k}, \bar{u}_{\ell|k})$, where $\bar{u}_{1|k}, \dots, \bar{u}_{\ell|k}$ is given by the solution of the previous iteration of the optimization, which is used to drive the nonlinear dynamics (9) initialized at the estimated state \hat{x}_k through Two-Step Unscented Kalman Filter [14, Sec. III] based on the measurement y_k to produce $\bar{x}_{1|k}, \dots, \bar{x}_{\ell|k}$. First, the continuous-time nonlinear dynamics are linearized with a zero disturbance assumption by defining

$$A_{c,j|k} \triangleq [\Delta f_x(\bar{x}_{j|k}, \bar{u}_{j|k}, p_1) \cdots \Delta f_x(\bar{x}_{j|k}, \bar{u}_{j|k}, p_n)], \quad (11)$$

$$B_{c,j|k} \triangleq [\Delta f_u(\bar{x}_{j|k}, \bar{u}_{j|k}, p_1) \cdots \Delta f_u(\bar{x}_{j|k}, \bar{u}_{j|k}, p_m)], \quad (12)$$

$$C_{j|k} \triangleq [\Delta g_x(\bar{x}_{j|k}, \bar{u}_{j|k}, p_1) \cdots \Delta g_x(\bar{x}_{j|k}, \bar{u}_{j|k}, p_n)], \quad (13)$$

$$D_{j|k} \triangleq [\Delta g_u(\bar{x}_{j|k}, \bar{u}_{j|k}, p_1) \cdots \Delta g_u(\bar{x}_{j|k}, \bar{u}_{j|k}, p_m)], \quad (14)$$

where $A_{c,j|k} \in \mathbb{R}^{n \times n}$, $B_{c,j|k} \in \mathbb{R}^{n \times m}$, $C_{j|k} \in \mathbb{R}^{p \times n}$, $D_{j|k} \in \mathbb{R}^{p \times m}$, and for all $i = 1, \dots, n$,

$$\Delta f_x(\bar{x}_{j|k}, \bar{u}_{j|k}, p_i) \triangleq \frac{[f(\bar{x}_{j|k} + p_i e_i, \bar{u}_{j|k}, 0) - f(\bar{x}_{j|k}, \bar{u}_{j|k}, 0)]}{p_i}, \quad (15)$$

$$\Delta g_x(\bar{x}_{j|k}, \bar{u}_{j|k}, p_i) \triangleq \frac{[g(\bar{x}_{j|k} + p_i e_i, \bar{u}_{j|k}, 0) - g(\bar{x}_{j|k}, \bar{u}_{j|k}, 0)]}{p_i}, \quad (16)$$

$p_i \in \mathbb{R}$ and $e_i \in \mathbb{R}^n$ are the perturbation magnitude and the standard basis vectors, respectively, and for all $i = 1, \dots, m$,

$$\Delta f_u(\bar{x}_{j|k}, \bar{u}_{j|k}, j, p_i) \triangleq \frac{[f(\bar{x}_{j|k}, \bar{u}_{j|k} + p_i e_i, 0) - f(\bar{x}_{j|k}, \bar{u}_{j|k}, 0)]}{p_i}, \quad (17)$$

$$\Delta g_u(\bar{x}_{j|k}, \bar{u}_{j|k}, j, p_i) \triangleq \frac{[g(\bar{x}_{j|k}, \bar{u}_{j|k} + p_i e_i, 0) - g(\bar{x}_{j|k}, \bar{u}_{j|k}, 0)]}{p_i}, \quad (18)$$

$e_i \in \mathbb{R}^m$ are the perturbation magnitude and the standard basis vectors, respectively, $\Delta f_x(\cdot), \Delta f_u(\cdot) \in \mathbb{R}^n$, and $\Delta g_x(\cdot), \Delta g_u(\cdot) \in \mathbb{R}^p$. We choose $p_i = 1e-8$ for all i . Next, define

$$M \triangleq \begin{bmatrix} A_{c,j|k} & B_{c,j|k} \\ 0_{m \times n} & 0_{m \times m} \end{bmatrix} \in \mathbb{R}^{(n+m) \times (n+m)}, \quad E \triangleq e^{Mt_{s,j}}, \quad (19)$$

then the discretized counterparts of the matrices $A_{c,j|k}, B_{c,j|k}$, are given by $A_{j|k} \triangleq E A$, $B_{j|k} \triangleq E B$, where E_A is the submatrix formed by the first n rows and first n columns of E , and E_B is the submatrix formed by the first n rows and the last m columns of E .

Thus, for all $j = 1, \dots, \ell$, the discretized and approximately linearized dynamics about the trajectory

$(\bar{x}_{1|k}, \bar{u}_{1|k}), \dots, (\bar{x}_{\ell|k}, \bar{u}_{\ell|k})$, are given by

$$x_{j|k} - \bar{x}_{j|k} = A_{j-1|k}(x_{j-1|k} - \bar{x}_{j-1|k}) + B_{j-1|k}(u_{j-1|k} - \bar{u}_{j-1|k}), \quad (20)$$

$$y_{j|k} - \bar{y}_{j|k} = C_{j|k}(x_{j|k} - \bar{x}_{j|k}) + D_{j|k}(u_{j|k} - \bar{u}_{j|k}), \quad (21)$$

where $\bar{x}_{0|k} \triangleq x_k$ and $\bar{u}_{0|k} \triangleq u_k$.

C. Quadratic Programming

In order to track the reference by penalizing the input move size and the given constraint violation with relaxation through the horizon, at each step k , the predicted control $u_{1|k}$ is obtained by solving the QP minimization

$$\min_{X_{1|k}, \varepsilon} (Y_{t,1|k} - R_{1|k})^T Q_t (Y_{t,1|k} - R_{1|k}) + \Delta U_{1|k}^T R_t \Delta U_{1|k} + \varepsilon^T S \varepsilon, \quad (22)$$

subject to

$$-F_{1|k} X_{1|k} = X_0, \quad (23)$$

$$\mathcal{C}_\ell Y_{c,1|k} + \mathcal{D}_\ell \varepsilon \leq \varepsilon, \quad (24)$$

$$U_{\min} \leq U_{1|k} \leq U_{\max}, \quad (25)$$

$$\Delta U_{\min} \leq \Delta U_{1|k} \leq \Delta U_{\max}, \quad (26)$$

where

$$X_{1|k} \triangleq \begin{bmatrix} x_{1|k}^T & u_{1|k}^T & \cdots & x_{\ell|k}^T & u_{\ell|k}^T \end{bmatrix}^T \in \mathbb{R}^{\ell(m+n)}, \quad (27)$$

where for all $j = 1, \dots, \ell$, $y_{t,j|k} \triangleq C_t y_{j|k} \in \mathbb{R}^{p_t}$, $Q_j \in \mathbb{R}^{p_t \times p_t}$ are the tracking-output weights, $R_j \in \mathbb{R}^{m \times m}$ are the control move size weights,

$$Y_{t,1|k} \triangleq \begin{bmatrix} y_{t,1|k} \\ \vdots \\ y_{t,\ell|k} \end{bmatrix} \in \mathbb{R}^{\ell p_t}, \quad R_{1|k} \triangleq \begin{bmatrix} r_{1|k} \\ \vdots \\ r_{\ell|k} \end{bmatrix} \in \mathbb{R}^{\ell p_t}, \quad (28)$$

$$Q_t \triangleq \begin{bmatrix} (\frac{t_{s,1}}{t_{s,1}})^2 Q_1 & \cdots & 0 \\ \vdots & \ddots & \vdots \\ 0 & \cdots & (\frac{t_{s,\ell}}{t_{s,1}})^2 Q_\ell \end{bmatrix} \in \mathbb{R}^{\ell p_t \times \ell p_t}, \quad (29)$$

$$R_t \triangleq \begin{bmatrix} (\frac{t_{s,1}}{t_{s,1}})^2 R_1 & \cdots & 0 \\ \vdots & \ddots & \vdots \\ 0 & \cdots & (\frac{t_{s,\ell}}{t_{s,1}})^2 R_\ell \end{bmatrix} \in \mathbb{R}^{\ell m \times \ell m}, \quad (30)$$

$$\mathcal{C}_\ell \triangleq I_\ell \otimes (\mathcal{C} C_c) \in \mathbb{R}^{\ell n_c \times \ell p}, \quad \mathcal{D}_\ell \triangleq 1_{\ell \times 1} \otimes \mathcal{D} \in \mathbb{R}^{\ell n_c}, \quad (31)$$

$$U_{1|k} \triangleq \begin{bmatrix} u_{1|k}^T & \cdots & u_{\ell|k}^T \end{bmatrix}^T \in \mathbb{R}^{\ell m}, \quad (32)$$

$$U_{\min} \triangleq 1_{\ell \times 1} \otimes u_{\min} \in \mathbb{R}^{\ell m}, \quad U_{\max} \triangleq 1_{\ell \times 1} \otimes u_{\max} \in \mathbb{R}^{\ell m}, \quad (33)$$

$$\Delta U_{\min} \triangleq 1_{\ell \times 1} \otimes \Delta u_{\min} \in \mathbb{R}^{\ell m}, \quad (34)$$

$$\Delta U_{\max} \triangleq 1_{\ell \times 1} \otimes \Delta u_{\max} \in \mathbb{R}^{\ell m}, \quad (35)$$

$$\Delta U_{1|k} \triangleq \begin{bmatrix} u_{1|k} - u_k \\ u_{2|k} - u_{1|k} \\ \vdots \\ u_{\ell|k} - u_{\ell-1|k} \end{bmatrix} \in \mathbb{R}^{\ell m}, \quad S = \mu_s I_{\ell n_c}, \quad (36)$$

$\mu_s \in \mathbb{R}$ is the slack weight. Note that (23) is an equality constraint that is satisfied if $x_{i+1|k} = A_{i|k}x_{i|k} + B_{i|k}u_k$ for all $i = 1, \dots, \ell - 1$, and is expressed in terms of

$$F_{1|k} \triangleq \begin{bmatrix} \bar{I}_x & \bar{0}_n & \cdots & \bar{0}_n & \bar{0}_n \\ N_{1|k} & \bar{I}_x & \cdots & \bar{0}_n & \bar{0}_n \\ \vdots & \vdots & \ddots & \vdots & \vdots \\ \bar{0}_n & \bar{0}_n & \cdots & \bar{I}_x & \bar{0}_n \\ \bar{0}_n & \bar{0}_n & \cdots & N_{\ell-1|k} & \bar{I}_x \end{bmatrix} \in \mathbb{R}^{\ell n \times \ell(m+n)}, \quad (37)$$

$$X_0 \triangleq \begin{bmatrix} A_{0|k}x_k + B_{0|k}u_k \\ 0_{\ell(n-1) \times 1} \end{bmatrix} \in \mathbb{R}^{\ell n}, \quad (38)$$

$$\bar{0}_n \triangleq 0_{n \times (m+n)}, \quad \bar{I}_x \triangleq [-I_n \ 0_{n \times m}] \in \mathbb{R}^{n \times (m+n)}, \quad (39)$$

where for all $i = 1, \dots, \ell - 1$,

$$N_{i|k} \triangleq [A_{i|k} \ B_{i|k} \ -I_n \ 0_{n \times m}] \in \mathbb{R}^{n \times 2(m+n)}. \quad (40)$$

VI. NUMERICAL SIMULATIONS

This section investigates the effects of model mismatch and disturbance on open-loop vibrational stabilization (VS) and closed-loop NMPC using numerical simulations. We also investigate the control effort required by each method by comparing input signal power. We assume that we have sampled and noisy measurements of θ and z and thus, $[y_{t,k} \ y_{c,k}]^T \triangleq [\theta(kT_s) \ z(kT_s)]^T + v_k$. The control u_k is the vertical base acceleration in m/s^2 . We set $r_k \equiv 0$ for stabilization. For all of the examples we apply NMPC with the parameters listed in Table I. For all of the examples

TABLE I: NMPC Parameters, descriptions, and values.

Parameter	Description	Value
T_s	Sample time	0.005 s/step
ℓ	Prediction horizon	10
$t_{s,1}, \dots, t_{s,\ell}$	Horizon breakup	$\text{linspace}(T_s, 2\ell T_s, \ell)$
p_i	Linearization perturbation	10^{-8}
(u_{\min}, u_{\max})	Control magnitude limits	$(-1500, 1500) \text{ m/s}^2$
$(\Delta u_{\min}, \Delta u_{\max})$	Control move size limits	$3 \cdot (-10^5, 10^5) \text{ m/s}^3$
z_{lim}	Base displacement limit	0.5 m
Q_i	Tracking-output weights	10^4
R_i	Control move size weights	10^{-4}
S	Slack weight	$10^9 I_\ell$
Q_F	Process Covariance	$3.4907 \times 10^{-5} I_n$
	Matrix (UKF)	
R_F	Measurement Covariance	$[2.6180 \times 10^{-5}]$
	Matrix (UKF)	10^{-3}
p_F	Initial Covariance	1
	Amplitude (UKF)	
α	Sample Weighting	1.2
	Parameter (UKF)	

we consider the KP model (2)–(4) where $g = 9.81 \text{ m/s}^2$, $l = 0.2485 \text{ m}$, $m = 1 \text{ kg}$, and $b = 0.0628 \text{ kg/s}$, unless stated otherwise. It can be shown that with these choice of parameters, the linearized KP dynamics have a 1 Hz natural frequency and the damping ratio 0.01. Note that the base displacement limit z_{lim} is selected to reflect the maximum amplitude of base displacement required by VS for KP with the given parameters. Note that unstable responses are clipped in plots. A nonuniform horizon with increasing step sizes is selected in order to capture a longer interval of time

without increasing the optimization complexity. Smaller step sizes closer to the present time step facilitate more accurate computations of u_{k+1} .

Example 1. *Vibrational and closed-loop stabilization of KP.* For VS, we consider $(\varepsilon, \delta) = (1.5, -0.7)$ on the Ince-Strutt diagram in Figure 2. The value of (ε, δ) correspond to an amplitude and frequency of base acceleration given by (5) and (7), respectively. In order to facilitate comparison, the values of (ε, δ) are selected so that the resulting amplitude of the base acceleration is similar to the output constraint on z in NMPC.

Figure 4 shows VS for a pair of (ε, δ) and closed-loop stabilization using NMPC. Figure 4 also shows that the asymptotic angle error with closed-loop stabilization is smaller than that with VS. Moreover, the NMPC base displacement is asymptotically smaller in magnitude than the vibrational control signal. Furthermore, NMPC reduces the command-following error faster than VS.

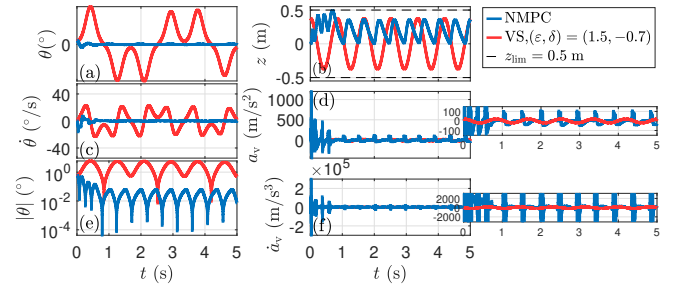


Fig. 4: Example 1: Stabilization of KP using NMPC with the parameters in Table I and using VS for given (ε, δ) pairs. (a) shows the angle of the pendulum; (b) shows the base displacement; (c) shows the angular velocity of the pendulum; (d) shows the base acceleration; (e) shows the absolute angle error; and (f) shows the base jerk. (d) and (f) have their magnified sections on the right hand side.

Example 2. *Effect of Initial Conditions* This example investigates the domain of attraction of VS and NMPC relative to the initial angle $\theta(0)$. Figure 6 shows that for $\theta_0 = 0.57^\circ$ VS stabilizes KP for all values of (ε, δ) within the theoretical boundary, however, for $\theta_0 = 10^\circ$ VS stabilizes KP for significantly fewer values of (ε, δ) . Figure 6(b) shows the largest values of $\theta(0)$ versus ε for two values of δ for which VS asymptotically stabilizes KP. Figure 7 shows that NMPC stabilizes KP with $\theta(0) = \pm 74^\circ$, whereas it is unable to stabilize KP for with $\theta(0) = \pm 80^\circ$. Thus, NMPC has a larger domain of attraction than VS with respect to the initial angle $\theta(0)$ of KP.

Example 3. *Effect of model mismatch.* This example investigates the effect of model mismatch on VS and NMPC. In particular, we simulate KP with 10% and 50%, of the pendulum length relative to the model used in NMPC and used to determine the (ε, δ) for VS. Figures 8(a) and (b) show that NMPC with erroneous models stabilizes KP, whereas VS

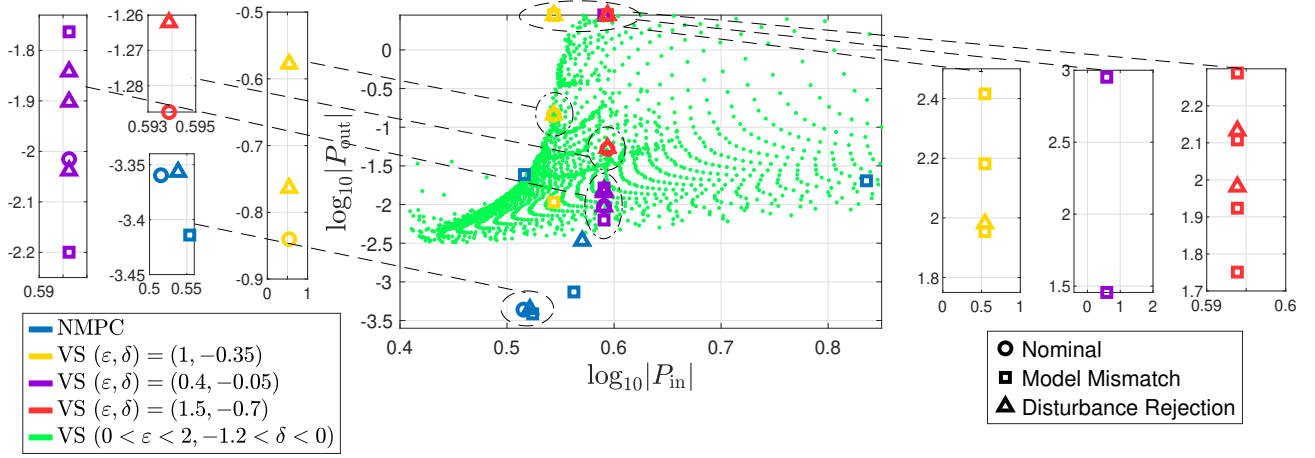


Fig. 5: Example 5: Output versus input signal power for VS and NMPC.

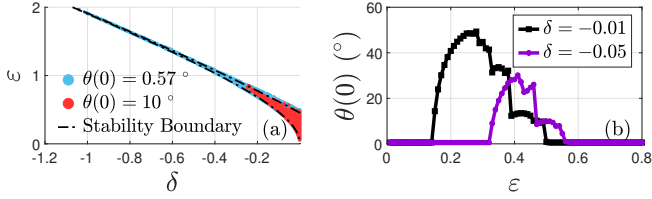


Fig. 6: Example 2: (a) blue and red dots denote values of (ε, δ) for which the numerically simulated KP (2)–(4) is stable under VS for $\theta(0) = 0.57^\circ$ and $\theta(0) = 10^\circ$, respectively; (b) shows the largest values of $\theta(0)$ for which VS is stabilizing versus ε for $\delta = -0.01$ and $\delta = -0.05$.

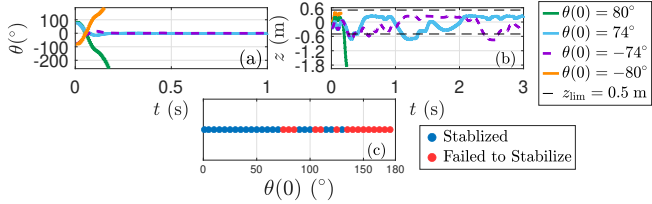


Fig. 7: Example 2: For NMPC, (a) show the pendulum angle θ , (b) shows base position z , (c) shows the largest possible stabilizing and destabilizing initial angles $\theta(0)$.

fails to stabilize KP for some combinations of model mismatch and (ε, δ) . \diamond

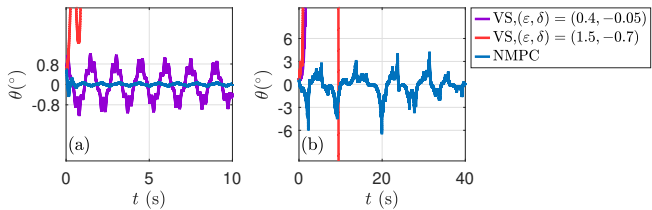


Fig. 8: Example 3: Stabilization of KP with VS and NMPC with model pendulum length mismatch of (a) +10%; (b) +50%. The plots are clipped and thus do not show demonstrate diverging signals.

Example 4. *Effect of noise and disturbance.* This example investigates the effect of zero-mean white Gaussian

sensor noise and torque disturbance on VS and NMPC. We simulate four cases

- i) $v_k \sim \mathcal{N}(0, \text{diag}([0.0001^2 \ 0.02^2]))$ and $w_k \equiv 0$,
- ii) $v_k \equiv 0$ and $w_k \equiv -0.005$,
- iii) $v_k \equiv 0$ and $w_k = 0.01 \sin 0.0157k$,
- iv) $v_k \equiv 0$ and $w_k \sim \mathcal{N}(0, 0.001^2)$.

Figure 9 shows that NMPC stabilizes KP for all four cases. The signal to noise ratio for angle and base position is < 20 dB for case 1 shown in Figure 9(a). Note that VS does not use sensors and is not affected by sensor noise in case 1. Figures 9(b) and (d) show that VS fails to stabilize KP for cases 2 and 4, respectively. \diamond

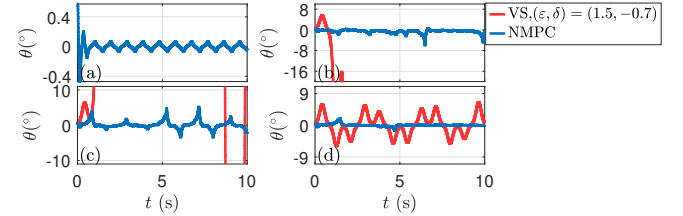


Fig. 9: Example 4: Stabilization of KP with VS and NMPC with (a) sensor noise, (b) fixed torque disturbance, (c) sinusoidal torque disturbances, and (d) zero-mean white Gaussian.

Example 5. *Signal Power Efficiency of NMPC.* This example investigates the relation between the input signal power and the output signal power of the VS and NMPC. We define $P_{\text{in}} \triangleq \sum_{i=1}^N \frac{|z(iT_s)|^2}{N}$ and $P_{\text{out}} \triangleq \sum_{i=1}^N \frac{|\dot{\theta}(iT_s)|^2}{N}$, where N is the number of data points in each simulation. Figure 5 shows $\log_{10}|P_{\text{out}}|$ versus $\log_{10}|P_{\text{in}}|$ for simulations with no model mismatch or disturbance, model mismatch, and disturbance. Note that in general simulations corresponding to NMPC has smaller values of $\log_{10}|P_{\text{out}}|$ than simulations with VS. Furthermore, several simulations corresponding to NMPC have smaller values of $\log_{10}|P_{\text{in}}|$ than simulations with VS. This demonstrates that in general NMPC requires less control power and wastes less power vibrating the pendulum than VS. \diamond

VII. CONCLUSIONS

In this paper, we explored the feasibility of applying an output-feedback nonlinear model predictive controller (NMPC) to the Kapitza pendulum (KP) stabilization problem. We demonstrated that NMPC stabilizes KP with less control effort than open-loop vibrational stabilization (VS) in several cases. Furthermore, we demonstrated that NMPC is more robust to initial conditions, disturbances and modeling errors than VS. This suggests that NMPC is a practically viable alternative to VS.

FUNDING SOURCES

This research was supported by ONR under BRC grant N00014-18-1-2211.

REFERENCES

- [1] H. E. Taha, M. Kiani, T. L. Hedrick, and J. S. M. Greeter, "Vibrational control: A hidden stabilization mechanism in insect flight," *Science Robotics*, vol. 5, no. 46, p. eabb1502, 2020. [Online]. Available: <https://www.science.org/doi/abs/10.1126/scirobotics.abb1502>
- [2] J. M. Berg and I. M. Wickramasinghe, "Vibrational control without averaging," *Automatica*, vol. 58, pp. 72 – 81, 2015.
- [3] M. Levi and W. Weckesser, "Stabilization of the inverted linearized pendulum by high frequency vibrations," *SIAM Review*, vol. 37, pp. 219–223, 06 1995.
- [4] J. A. Blackburn, H. J. T. Smith, and N. Gronbech-Jensen, "Stability and hopf bifurcations in an inverted pendulum," *American Journal of Physics*, vol. 60, no. 10, pp. 903–908, 1992.
- [5] H. J. T. Smith and J. A. Blackburn, "Experimental study of an inverted pendulum," *American Journal of Physics*, vol. 60, no. 10, pp. 909–911, 1992. [Online]. Available: <https://doi.org/10.1119/1.17012>
- [6] N. Bhadra and S. Banerjee, "Dynamics of a system of coupled inverted pendula with vertical forcing," *Chaos, Solitons & Fractals*, vol. 141, p. 110358, 12 2020.
- [7] E. Butikov, "On the dynamic stabilization of an inverted pendulum," *American Journal of Physics*, vol. 69, 07 2001.
- [8] J. Baillieul and B. Lehman, *Open-loop control using oscillatory inputs*. CRC, 2018, pp. 1191–1211.
- [9] Z. Artstein, "The pendulum under vibrations revisited," *Nonlinearity*, vol. 34, pp. 394–410, 2021.
- [10] J. K. Hale, *Ordinary Differential Equations*. Wiley, 1969.
- [11] H. Khalil, *Nonlinear Systems*, 3rd ed. Pearson, 2014.
- [12] W. S. Levine, *The Control Systems Handbook, Second Edition: Control System Advanced Methods*, 2nd ed. USA: CRC, 2009.
- [13] A. A. Grandi, S. Protière, and A. Lazarus, "Enhancing and controlling parametric instabilities in mechanical systems," *Extreme Mechanics Letters*, vol. 43, p. 101195, 2021.
- [14] A. Goel and D. Bernstein, "On the Accuracy of the One-step UKF and the Two-step UKF," *arXiv:2208.09055*, 2022.